Influences of Dicumyl Peroxide on Morphology and Mechanical Properties of Polypropylene/Poly(styrene-*b*-butadiene-*b*-styrene) Blends via Vane-Extruder

Li Yang, Jintao Huang, Xiang Lu, Shikui Jia, Haichen Zhang, Gang Jin, Jinping Qu

National Engineering Laboratory for Plastic Modification and Processing, National Engineering Research Center of Novel Equipment for Polymer Processing, South China University of Technology, Guangzhou 510640, China
The authors declare no competing financial interest
Correspondence to: G. Jin (E-mail: pmrdd@scut.edu.cn) and J. Qu (E-mail: jpqu@scut.edu.cn)

ABSTRACT: Polypropylene (PP) and poly(styrene-*b*-butadiene-*b*-styrene) block copolymer (SBS) were melt-blended in the presence of initiator system. Dicumyl peroxide (DCP)/Triallyl isocyanurate (TAIC) via self-deigned VE, aiming at *in situ* reactive compatibilization of toughed PP/SBS blend. The reactivity, morphology and mechanical properties of PP/SBS/DCP/TAIC blends were studied. Online torque detection was conducted to monitor changes in viscosities of reactive compatibilized blends, which could give proof of the interfacial grafted reaction induced by DCP/TAIC system. The effect of reactive compatibilization on the dispersed particles sizes and interfacial adhesion was studied by scanning electron microscopy. Analysis on mechanical performance revealed the impact strength improved after treated by initiator system, moreover, the impact-fractured surface observation showed, the failure mode changed from debonding mechanism of neat 50PP/50SBS blend to plastic deformation mechanism of blend containing 3.0 phr initiator system. With improved interfacial adhesion, compatibilized blends not only were toughened but also exhibited enhanced tensile strength and thermal stability. Dynamic mechanical analysis showed a reduction of ΔT_g between PP phase and the PB segments in SBS phase, indicating reactive compatibilization of the blend was achieved. In the final part, a brief discussion was given about the dominant effects from chain scission of PP matrix to intergrafting reactions of PP and SBS, under different content of DCP/TAIC initiator system. © 2014 Wiley Periodicals, Inc. J. Appl. Polym. Sci. **2015**, *132*, 41543.

INTRODUCTION

Polypropylene (PP) has an important place among the synthetic polymers because of its growing commercial applications in many consumer and engineering fields. However, its application as a structural material is limited because of its relatively low impact resistance. One most extensive researched way to solve this problem is blending (toughening) of PP with elastomers,[1–3] usual impact modifiers for the PP are olefinic copolymers based on ethylene and propylene (EPR, mEPR, EBR, POE, or EPDM[4,5]), as well as styrenic rubber block copolymers (SRBC or SBC: SBR, SBS, SIS, SEP, SEBS).[6,7] This article is focused on the blends of PP and poly(styrene-*b*-butadiene-*b*-styrene) block copolymer (SBS). However, although the molecular chains of PP and elastomers are similar, PP/rubber blends are mostly immiscible because of unfavorable interactions between the molecular segments of PP and the elastomers, which will result in a phase-separated morphology. Lacking of interfacial adhe-sion in the solid state lead to a deterioration in properties, particularly for those related to ductility. Therefore, numerous studies have been done to modify the morphology to increase the compatibility between the two phases that leads to the mod-ification of morphology.

One way to improve the compatibility of PP/SBS blends is to use a block or graft copolymer,[8,9] which contains segments of chains capable of specific interactions or chemical reactions with the blend components. Wilhelm and Felisberti[10] have studied the morphology and mechanical properties of blends of isotactic PP (i-PP) and a maleated styrene–butadiene–styrene triblock copolymer with maleic anhydride (SBS–MAH), the i-PP/SBS–MAH blends showed an impact strength superior to that of the corresponding i-PP/SBS blends, which was attributed to the formation of the graft copolymer during the melt blend-ing. Hernández et al.[11] had prepared dynamically vulcanized PP/SBS blends, and Deeply Double Edged Notched Tension

specimens were cut from injection molded plaques for fracture testing. The fracture behavior of dynamically vulcanized thermoplastic/elastomer (PP/SBS) blends by means of the essential work of fracture approach was investigated. They found that the dynamic vulcanization method can impair fracture resistance to PP/SBS blends. Madhumita Saroop et al.[12] had prepared unvulcanized and dynamically vulcanized blends of isotactic PP and SBS by a modified phenolic resole resin in an internal mixer. After evaluation of mechanical properties, they found the dynamically vulcanized PP/SBS blends showed higher impact strength, yield stress, and percent elongation than the corresponding unvulcanized blends.

However, *in situ* reactive compatibilization is preferred technologically compared to the addition of a specially tailored, usually expensive, copolymer.[13,14] It has been applied by several authors in compatibilization of PP with various elastomer polymers in bids to improve its toughness.[15–17] In this work, *in situ* reactive compatibilization of PP and SBS block copolymer, was achieved in the presence of an initiator, dicumyl peroxide (DCP). DCP is a kind of peroxide free radical initiator, mainly used as a polymerization initiator, a vulcanizing agent of natural rubber, synthetic rubber, also used as crosslinking agents for polyethylene resin. As a free radical initiator, it has been used by several researchers to induce *in situ* reaction between components in polymer blends.[18,19] Kristine et al.[20] have used 1% hexa(allylamino)cyclophosphonitrile (HAP) and peroxide during reactive extrusion for PP/EPDM. They have observed an increase in low-temperature impact strength and an enhanced dispersion of EPDM in the PP matrix in the presence of peroxide and HAP as new multifunctional coupling agent. Kim et al.[21] have used poly(ethylene-comethacrylic acid) as ionomer and have applied dynamic vulcanization to control miscibility of the PP/EPDM blends. Their results have demonstrated that the dynamic vulcanized PP/EPDM blend containing 15 wt % of Zn-neutralized ionomer and 1.0 phr DCP leads to thermoplastic interpenetrating polymer networks structure and leads to enhancement of the blend miscibility. To the best of our knowledge, few works had investigated the reactive compatibilization of PP/SBS blend in the presence of a peroxide initiator. Therefore, it is the objective of the current study to prepare toughened PP/SBS blends in a reaction with DCP, to study the compatibilization effects after characterization and relate the morphology to the properties of the blends. This is an important issue in designing PP based toughing materials.

In this article, immiscible binary blend of PP and SBS elastomer was extruded via vane-extruder (VE) designed by professor Qu in South China University of Technology, Guangzhou, China. As we know, in polymer processing, the elongation flow is more effective than the shear flow. Several studies have reported that melt drops in polymer processing are more efficiently broken under elongation flow than under shear flow.[22–24] Various attempts have been performed to generate elongation flow based on converging channels, but most of these elongation flows are local and fixed.[25–27] Qu[28] invented a novel nonscrew plasticizing processing tool known as the VE, which consists of certain groups of vane plasticizing units and can generate higher stress and dynamic elongation flow. The elongation flow is more

effective possibly because the positive displacement-type flow dominates the solid conveying mechanism of VE. Moreover, the solids are compact and transported regardless of their material properties, which can remarkably shorten the thermomechanical history of the material and improve the suitability of polymer processing.[29] These will reduce macromolecule chain damage. Compared with screw extruder, VE showed better mechanical properties and finer dispersion particles because of the positive displacement-type characteristics of solids conveying.[30]

After the extrusion of binary blend, DCP was introduced into the system. Covulcanizing agent triallyl isocyanurate (TAIC) was used to improve the crosslinking efficiency from controlling the degradation reaction,[31,32] remarkably decrease the probability of PP chains scission during blending. The reactive compatibilization effect of the initiator system (DCP/TAIC) on the binary system was studied. This job would make a contribution to the broaden application of reactive compatibilized plastic/elastomer blends on the VE.

EXPERIMENTAL

Materials

PP (T30S, density = 0.9 g/cm^3, MFI = 2.9$\sim$3.5 g/10 min, T_g = 15.5°C) was provided by Daqing Petrochemical (China). Poly(styrene-*b*-butadiene-*b*-styrene) (SBS, YH-792, S/B = 40/60, density = 0.92–0.95 g/cm^3, MFI = 5.0–5.5 g/10min, T_{g1} = −87.0°C, T_{g2} = 95.0°C) was provided by Baling Petrochemical (China). DCP (Cas 80-43-3, Chemical pure = 99.5%) with typical half-life time about 1 min at 171°C was purchased from Chengdu Kelong Chemical Reagent, China. TAIC (Cas 1025-15-6, Analytical reagent = 99%) was purchased from local chemical plant. Ethanol absolute (C$_2$H$_5$OH % > 99.7%, density at 20°C = 0.789–0.791 g/cm^3) was supplied by Tianjin Fuyu Fine Chemical (China). Toluene (Cas 108-88-3, density = 0.87 g/cm^3) from Shanghai Chemical Reagent Company, China.

Composition and Abbreviation of Samples

The composition and abbreviation of different samples are presented in Table I. The content of SBS in binary blend are 5, 15, 30, and 50 wt %, for further study of the reactive compatibilization of PP/SBS blends with initiator system, sample PP/SBS (50/50) (E#) was chosen as the matrix into which different content of DCP/TAIC system were introduced. The DCP content in "phr" was settled with reference to 100 parts of SBS elastomer, for sample 3# 50 g PP/50 g SBS, 3.0 phr mean 1.5 g of DCP. The ratio of DCP/TAIC was fixed at 2/1, which was thought will contribute the best processability and properties of polymer blends according to Refs. [33 and [34].

Preparation of Neat and Compatibilized Blends

Before experiments, The PP, SBS particulates were dried at 80°C for 4 h in an air oven to avoid possible moisture-degradation reactions. According to Table I, the prepared samples with determined content were manually premixed by tumbling in a plastic zip–lock bag, and subsequently fed into the VE at a screw speed of 30 r/min. The temperature profiles of the barrel were 120–180-180-180-180°C from hopper to the die. Main processing parameters of VE in this experiment are shown in Table II. All the extruded rods were cooled in a water bath

Table I. Composition and Abbreviation of Binary Blends and Reactive Blends

Samples	PP (g)	SBS (g)	DCP (g)	TAIC (g)	DCP content (phr)	DCP/TAIC ratio
A[#]	100	0	0	0	0	0
B[#]	95	5	0	0	0	0
C[#]	85	15	0	0	0	0
D[#]	70	30	0	0	0	0
E[#]	50	50	0	0	0	0
1[#]	50	50	0.5	0.25	1.0	2/1
2[#]	50	50	1.0	0.50	2.0	2/1
3[#]	50	50	1.5	0.75	3.0	2/1

immediately, and a pelletizer was used to cut the extrudates into pellets. Finally, the pellets were dried in an air oven for 4 h at 80°C for injection molding. The injection molding was carried out in a plastic injection molding machine (HTB110X/1, China) to obtain tensile and impact specimens for observations. The barrel temperature profiles of the injection molding were 210–200–200–180°C, the injection pressure was 25 MPa, dwell pressure was 30 MPa and the mold temperature was 30°C. The mixing time was 5 sec, the dwelling time was 6 sec and the cooling time was 5 sec.

CHARACTERIZATION

Online Torque Observation

The torque/time graph allows for dynamic evaluation of the change in viscosity during processing which was closely related to the reactions in the blends.[35,36] It had been reported that peroxide initiators have the ability to induce the vulcanization of rubber and degradation of PP chains.[37,38] To study the reactivity of DCP/SBS, DCP/PP and DCP/SBS/PP, experiments were conducted under the following three processing protocol: (i) SBS was separately melted in a Brabender Plasticorder with a chamber of 55 cm^3 for 2 min, then DCP/TAIC was added. When the torque value stayed stable for 1–2 min, finally PP particles were added into the system and the mixing was continued for 3–4 min; (ii) Similar to experiment (i), while PP was melted for 2 min first, then DCP/TAIC was added into the chamber. Allowing the torque value stayed stable for 1–2 min then SBS elastomer was added. Finally the mixing was continued for 3–4 min; (iii) Both PP and SBS particles were mixed melted in the mixer for 2 min, then DCP/TAIC was introduced to the blend. At last the mixing was continued to 6 min. During the three experiments, the rotor speed was 50 r/min and the temperature of the mixing chamber was set at 190°C.

IR Spectra

IR spectra of the blends were obtained from an American instructment (Nexus 670, Nicolet Company), which has 0.1–0.005 cm^{-1} resolution ratio. Before testing, the particles (parts of injection-molded products) were pressed into a film (0.03 mm) by two heated molds at 250°C. Then theses samples were measured at 400–4000 cm^{-1}.

SEM Observation

To estimate the domain sizes of dispersed-phase and the morphology of the blends with different content of DCP/TAIC, the injection-molded products (4 mm thick of rod) were submerged in liquid nitrogen for approximately 75 min and fractured to expose the internal structure for scanning electron microscope (SEM) investigations with a SEM (model HITACHI S-3700N, Japan). To better clarify the brittle–ductile transition of the blends containing different content of DCP/TAIC, the impact-fractured surfaces of different samples were also investigated by SEM. Before testing, all the specimens were gold-sputtered to provide enhanced conductivity. In some cases, the fracture surfaces were etched by toluene for 24 h to remove the soluble SBS phase.

Mechanical Properties

The injection molded specimens are 4 mm thick with a distance of 50 mm between grips were applied for tensile testing. The tensile properties were measured with a CMT 4204 universal testing machine (Shenzhen SANS Testing Machine, Shenzhen, China) at a cross-head speed of 50 mm/min according to the GB/T 1040-92 standard. Plates with 4 mm thick were used for impact testing. Instron POE2000 pendulum impact tester was used in impact test at room temperature (25°C). For all the mechanical property determination, five or more samples were tested, and then the results were averaged.

Dynamic Mechanical Analysis

Dynamic mechanical analysis (DMA) was performed with a Netzsch DMA242c instrument dynamic mechanical analyzer at a fixed frequency of 10 Hz and oscillation amplitude of 0.15 mm to provide the plots of the loss factor (tan δ) and the storage modulus against the temperature. The scans of the blends were carried out in a three-point bending mode at a

Table II. Main Processing Parameters of VE

Extruder	Number of VPCU	Rotor diameter, d (mm)	L/D	Productivity (kg/h)	Speed (rpm)	Processing temperature (°C)
VE	12	40	12	35	30	120-180-180-180-180
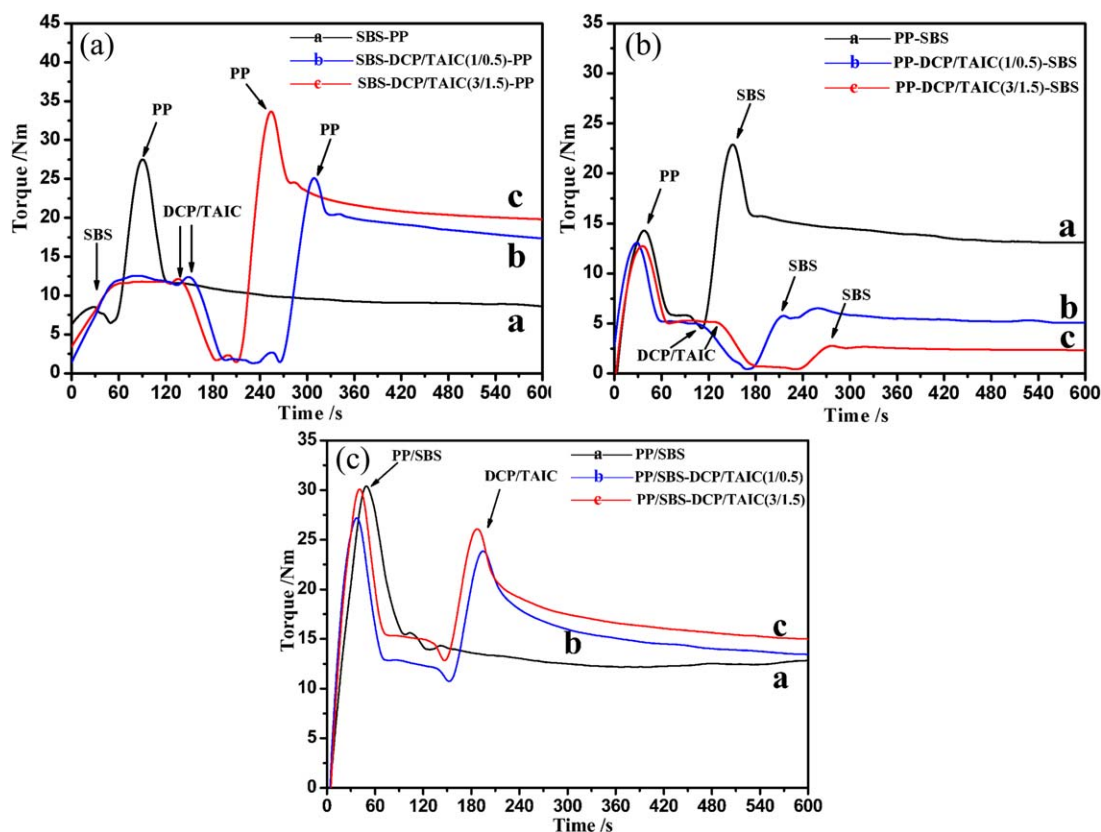
Figure 1. Torque evolutions for different mixing processes: (a) experiment (i), (b) experiment (ii) and (c) experiment (iii). [Color figure can be viewed in the online issue, which is available at wileyonlinelibrary.com.]

constant heating rate of 3°C/min and at a frequency of 1 Hz from −130 to 150°C.

Thermogravimetric Analysis

The particles (parts of injection-molded products) were applied for TGA testing. Thermogravimetric analysis (TGA) was performed on about 10 mg samples on a Netzsch TG209 instrument from 30 to 600°C in a N_2 atmosphere (250 mL/min) with a 10°C/min heating ramp. All thermal parameters provided were determined in an average of three repeats.

RESULTS AND DISCUSSION

In Situ Grafted Reaction observation

We took several experiments before studies to prove the concerning reactions on neat components with DCP given in. When PP was extruded with DCP alone, the viscosity of PP decreased sharply, melt quality was desperately weak. The melts could not even be pulled into extruded rods, let alone cutting into pellets and injection molded. PP/DCP blend didn't enjoy mechanical strength due to serious degradation of PP macromolecular. When SBS was extruded with DCP alone, SBS elastomers translated into rubber powders. SBS powders could not be molded for the molecular chains had been crosslinked. The reason was that SBS particles were vulcanized due to interaction of DCP with carbon double bond in soft SBS domains. These were what we had discovered before the whole study. These phenomena were also showed in the in the batch mixer (experiments i, ii).

During the mixing processes of experiment (i), the tracking of torque was shown as in Figure 1(a). Curve "*a*" in Figure 1(a) represented for the nonreactive binary mixing process, which mean SBS particles were first premixed in the chamber, then PP particles were introduced. The torque value of binary blend stayed stable at approximately 10 Nm. As one can see in curve "*b*" and "*c*" in Figure 1(a), once DCP/TAIC system was introduced into the chamber after SBS. The torque value showed a short increase then decreased sharply, then kept stable at 1.5 Nm. After that, the ram was opened for the next feeding of PP, inside the chamber, SBS melt appeared like spongy agglomerates. The reason of the great loss on torque could be due to the fact that DCP/TAIC initiative systems had induced a large extent of crosslinking reactions of SBS. Self-crosslinked SBS melts transferred into vulcanized solid rubber powders with higher density. The sharp decline in volume (from melts to solids) would result in a plunge of pressure for the rotor, thus exhibiting a sharp decline on torque curve. However, when PP was finally added, torque value increased to 18–19 Nm, even higher than that of neat SBS/PP blends (10 Nm). This final increment signified a further increase of melt viscosity, which could be the result of the intergrafting reaction between SBS and PP or the crosslinking of PP. For the real reason of final increment, experiment (ii) was conducted.

As shown in Figure 1(b) for experiment (ii), curve "*a*" also represented the nonreactive binary mixing process. While in this part, PP was melted first, followed by the mixing of SBS, the
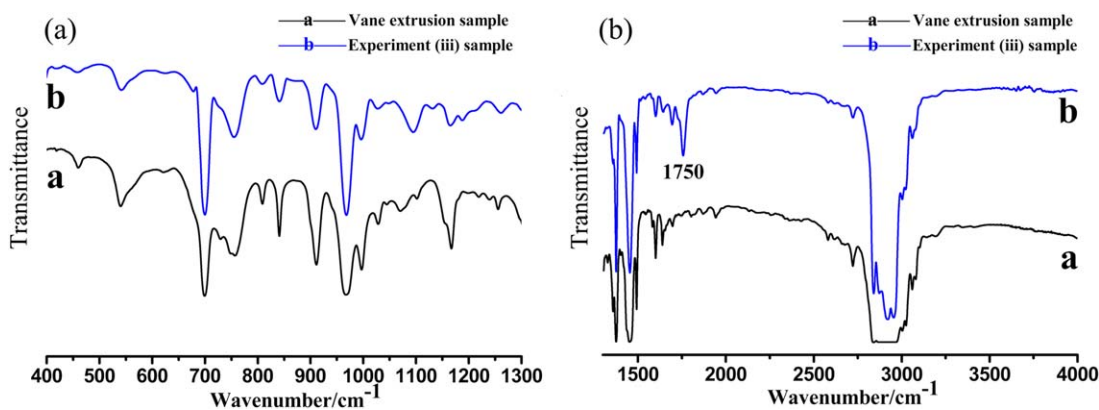
Figure 2. IR spectra of PP/SBS/DCP/TAIC (50/50/1.5/0.75) sample from experiment iii and vane-extrusion. [Color figure can be viewed in the online issue, which is available at wileyonlinelibrary.com.]

final torque value showed stable at 15 Nm. As for curve "*b*" and "*c*," when DCP/TAIC was introduced into PP melts at 2–3 min, a reduction in torque value showed, once the torque kept stable, low viscosity of PP melts could be found when the ram was opened for the next feeding. This could be attributed to the degradation of macromolecular chains of PP. From this we could make the conclusion, the final increase in Figure 1(a) (curve "*b*," "*c*") was the result from intergrafting reactions between SBS and PP, because chain scission would predominant over chain grafting on the presence of DCP/TAIC. The increase in the torque measured with the mixing time is indicative of the occurrence of chemical reactions between two phases initiated by DCP.

Experiment iii [Figure 1(c)] is quite different from the former two. Before modification by the initiators, the two components PP and SBS were melted together, aiming to monitor the processing condition in the VE. Figure 1(c) shows the tracking of torque during the mixing process of the PP/SBS (50/50) blend with different concentrations of DCP/TAIC. As opposed to the torque of the neat PP/SBS (50/50), which continuously decreased with time, the torque of PP/SBS/DCP/TAIC rose after the addition of initiators. With further mixing time, the system showed stable torque value at 15–18 Nm higher than that of physically blend (approximately at 13 Nm). This indicated an increased viscosity because of formation of interphase grafted structure. We also admitted the occurrence of vulcanization reaction of SBS phase and chain scission of PP phase during this process.

To confirm the mixing of experiment iii in the Brabender Plasticorder is comparable with that in the VE, we take IR spectra of the PP/SBS/DCP/TAIC (50/50/1.5/0.75) blends of experiment iii and vane-extrudates to analyze the chemical structure of these two. Before testing, samples were immersed in absolute ethanol for 24 h to eliminate remaining DCP and TAIC in the samples, which may bring some deviation to the IR results. As we can see in Figure 2, both in the functional group region [Figure 2(a)] and fingerprint region [Figure 2(b)], samples from Brabender Plasticorder and VE exhibited similar characteristic curves. The only extra peak in curve "*a*" at nearly 1750 cm^{-1} was possibly from the stretching of "C=O" groups in the remaining TAIC.

From these, we can see the results of experiment (i, ii, and iii) are referenceable for the processing and analyzing of the extrusion. Observations on torque curves gave direct evidence to the interphase grafting reaction between SBS and PP with the presence of initiator system DCP/TAIC. The formation of longer chains within the phases led to increases in the viscosities for the blends also will enhance the compatibility of the blend, which will be further studied in the following parts.

Phase Morphology

The phase morphologies of neat blends with various compositions of PP/SBS are shown in Figure 3. The neat blends of various compositions exhibited distinct "droplet" morphologies, heterogeneous distribution of sizes of the dispersed particles could be found, the smoothly debonding surfaces and empty holes indicated complete phase separation and immiscibility between elastomer SBS and plastic PP. This immiscible morphology expectedly became worse with increased SBS content, as one can see in Figure 3(d) (PP/SBS 50/50 blend), SBS particles agglomerated in the blend, particle sizes were highly uneven, more smoothly debonding surfaces and empty holes could be found, indicating poor interfacial adhesion between phases.

To discover the compatibilization effects, morphologies of compatibilized blends with various contents of DCP/TAIC system on same matrix of PP/SBS (50/50) are shown in Figure 4. Compared to neat blend, significant changes in fracture surfaces of reactive blends could be observed. As shown in Figure 4(b), the dispersed particle sizes were greatly reduced, uniform particle size of the dispersed phase could be found. The interface and empty holes became vague, all these showed an enhancement on the interfacial compatibility. The compatibilization effect became more obvious in Figure 4(d), which represented for the blends treated with 3.0 phr initiator system. As one can see, the interface between SBS and PP became vaguer, originally "droplet" morphology could not be found any more. This indicated a strong mutual-compatibility of two phases.

Fractured surfaces of selective etched SBS phase were shown in Figure 5, as shown in Figure 5(a), a lot of concave holes exist on the fracture surface of PP/SBS (50/50) blend. The sizes of
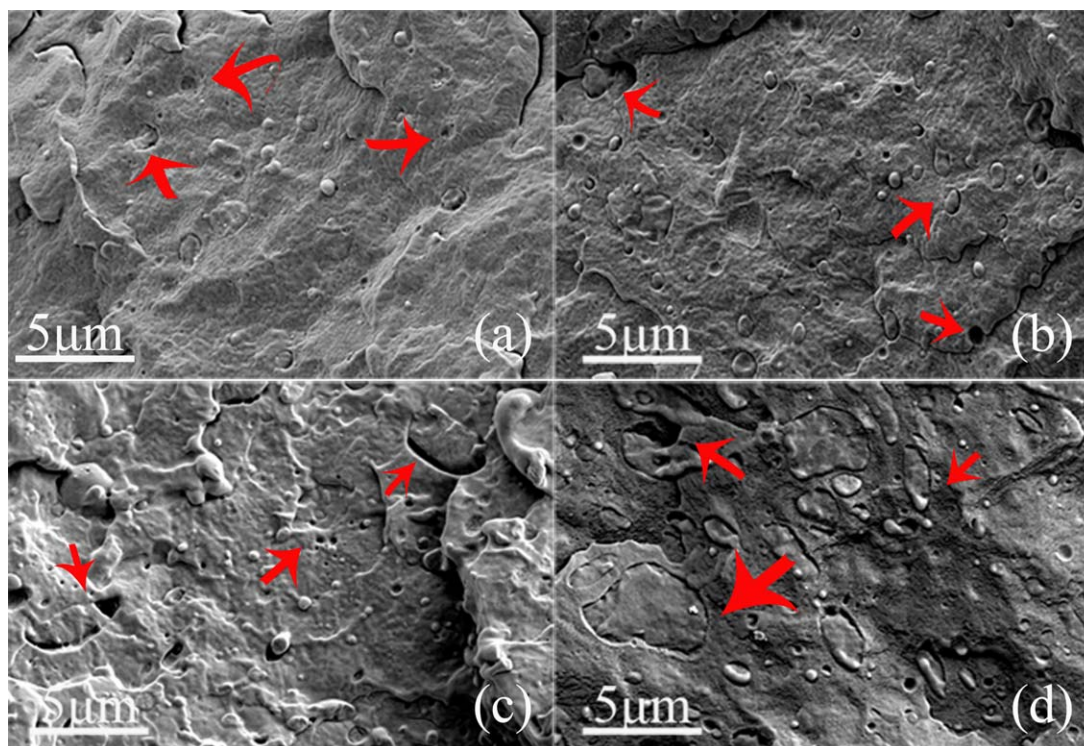
Figure 3. Morphology of the cryofractured surfaces: (a) PP/SBS (95/5), (b) PP/SBS (85/15), (c) PP/SBS (70/30), (d) PP/SBS (50/50). [Color figure can be viewed in the online issue, which is available at wileyonlinelibrary.com.]

the holes were highly uneven, the formation of these particles or holes should be related to the separation or pullout of SBS aggregates from PP matrix. The fracture surface of PP/SBS/

DCP/TAIC (50/50/1.0/0.5) [see Figure 5(b)] differed obviously from those of neat PP/SBS samples in that small amount of concave holes can be found on their fracture surfaces. The
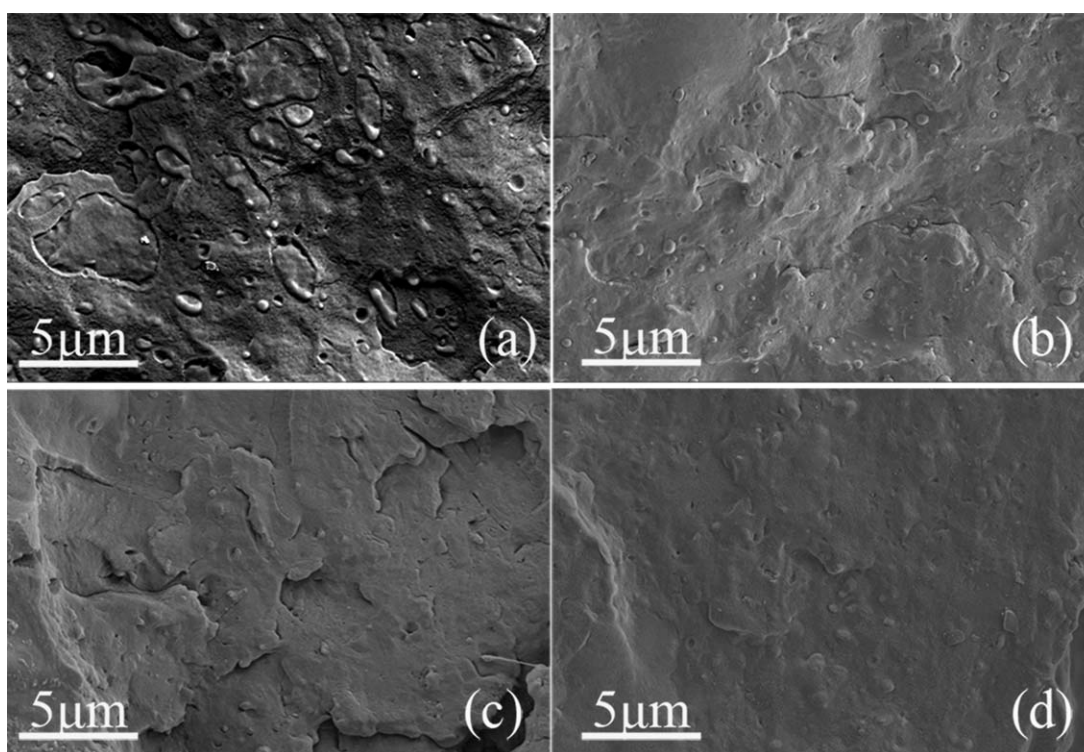
Figure 4. Morphology of the cryofractured surfaces: (a) PP/SBS (50/50), (b) PP/SBS/DCP/TAIC (50/50/0.5/0.25), (c) PP/SBS/DCP/TAIC (50/50/1.0/0.5), (d) PP/SBS/DCP/TAIC (50/50/1.5/0.75).
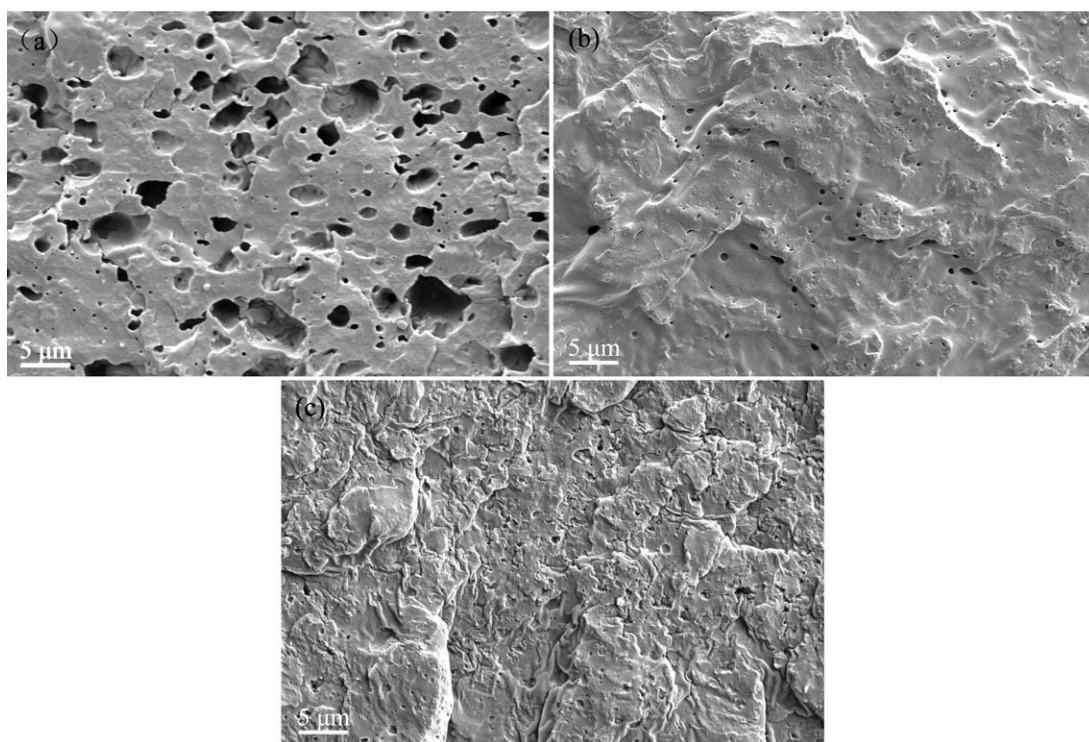
Figure 5. The etched surface morphologies: (a) PP/SBS (50/50), (b) PP/SBS/DCP/TAIC (50/50/0.5/0.25), (c) PP/SBS/DCP/TAIC (50/50/1.5/0.75).

diameter of holes decreased sharply, indicating less separated SBS particles in this sample. As for sample PP/SBS/DCP/TAIC (50/50/1.5/0.75) in Figure 5(c), significant changes occurred in the phase morphology. Originally "sea-island" morphology dis-appeared, no more etched holes of SBS could be found, suggest-ing crosslinking of SBS domains. Interfaces became vague, and great wrinkled convex domains could be observed in Figure 5(c), indicating large extent of grafted reaction.
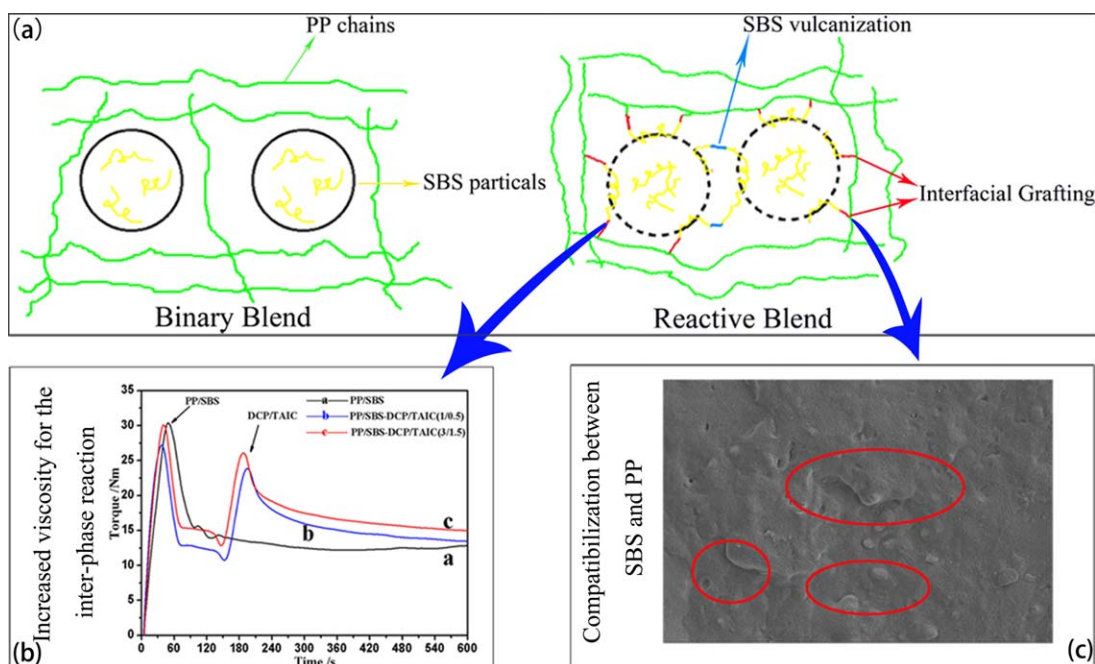
Figure 6. (a) "Cartoon" model depicting interphase grafting reaction, (b) torque/time graph for the neat PP/SBS blend and reactive blends showing increased viscosity, and (c) high magnification of cryofractured surface in Figure 3(d) showing integration of interface. [Color figure can be viewed in the online issue, which is available at wileyonlinelibrary.com.]

Table III. Mechanical Properties of Binary and Compatibilized Blends

Samples	Tensile strength (MPa)	Impact strength (kJ/m^2)	Elongation at break (%)
A$^\#$	32.44	4.39	107.16
B$^\#$	28.58	5.99	153.45
C$^\#$	26.78	6.90	170.20
D$^\#$	25.40	8.41	169.64
E$^\#$	22.62	11.51	222.14
1$^\#$	17.66	8.63	233.17
2$^\#$	16.55	6.83	124.10
3$^\#$	23.31	27.96	612.05

This modification on morphology has been attributed principally to two factors: (i) compatibilization between PP and SBS; (ii) alteration of the viscosity as a result of interphase grafting reaction during processing.[39] This concept is illustrated in the "cartoon model" in Figure 6. During reactive processing, free radical initiators would react with the active "β-C" in PP and the "C≡C" double-bond in SBS, resulting in a formation of *in situ* grafted copolymers, which acted as reactive compatibilizers.[20] It is the copolymers led to better interaction between SBS and PP, resulting in intergrated interfaces of PP and SBS. Part of the reason for the increase on viscosity of reactive compatibilized blends should be the formation of grafted copolymers. The crosslinking (self-vulcanization) of SBS domains could also make the melt hard to flow, although unwanted chain scission of PP might also occur.

Mechanical Properties

Mechanical properties of binary and compatibilized blends were listed in Table III. The tensile strength and elongation at break of neat PP/SBS (50/50) blend and reactive compatibilized blends are shown in Figure 7. For the reactive compatibilized system with lower contents of DCP/TAIC (1.0–2.0 phr), tensile strength and elongation at break showed a decrease from 22.62 MPa, 222.14% to 16.55 MPa and 124.1%, respectively. However, when
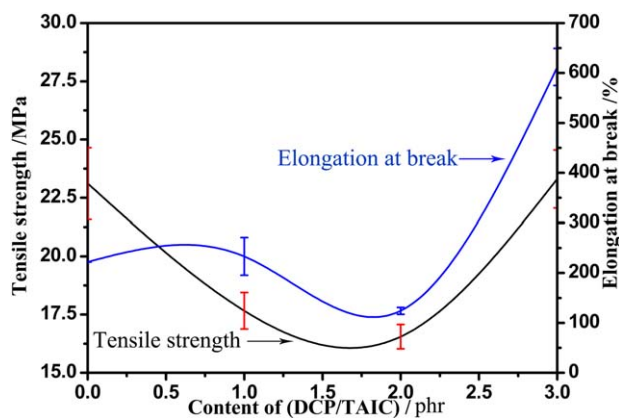
increasing the initiator system to 3.0phr, both these two properties increased remarkably to 23.31 MPa and 612.1%, respectively, higher than those of untreated binary blend PP/SBS (50/50). To observe the resistance to impact performance of these blends, we could find the same tendency. The notched impact strength of neat PP/SBS (50/50) blend and reactive compatibilized blends are shown in Figure 8. First, when modified by lower content of DCP/TAIC (1.0–2.0 phr), the impact strength suffered a loss from 11.51 to 6.83 kJ/m^2, then increased drastically to 27.83 kJ/m^2 after increasing the initiator system to 3.0 phr, over twice than that of PP/SBS (50/50) blend, nearly seven-times than that of pure PP.

As we can see, there was a transition from neat PP/SBS (50/50) blend to PP/SBS/DCP/TAIC (50/50/1.5/0.75). The tensile toughening mechanism in the polymer blends was ascribed to the yielding deformation of the matrix. In the same breadth, the improved resistance to impact in the blends is attributed to shear yielding of the matrix, which had been initiated by debonding microvoids. According to the model of micromechanical deformation in blends by Kim and Michler,[40] a three-stage process was envisaged: (i) stress concentration within the inclusion; (ii) void and shear band formation; (iii) induced shear yielding. Morphology of the impact-fractured surfaces of neat PP/SBS (50/50) and reactive compatibilized blends were shown in Figure 9. Because PP and SBS exhibit different resistances to impact, with the latter being tougher, the SBS particles could act as stress concentrators in the blends. This essentially converts the uniaxial stress to a triaxially concentrated stress that leads to volume dilation around the SBS particles.

For the neat blend, debonding easily occurred because of poor interphase adhesion, that's why we could find obvious cavities between dispersion particles and the matrix. According to the debonding mechanism,[41] cavities would lead to premature interfacial failure and hence rapid void propagation, only absorbing very little energy, thus exhibiting somewhat brittle failures. Conversely, for compatibilized blends in Figure 9(d), it could be
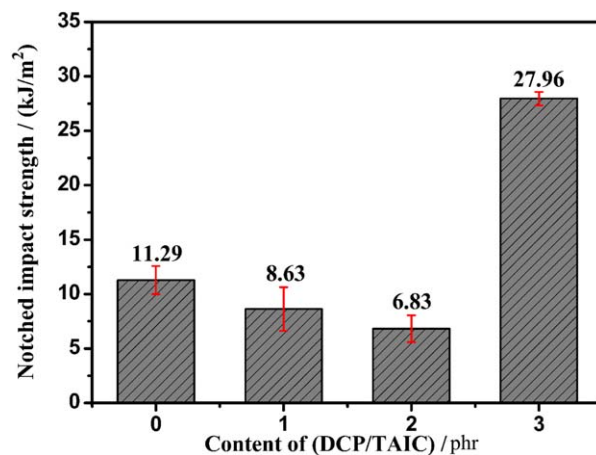

Figure 7. The tensile strength and elongation at break with variation in weight ratio of the DCP/TAIC content in the same matrix blends of PP/SBS (50/50). [Color figure can be viewed in the online issue, which is available at wileyonlinelibrary.com.]

Figure 8. The notched impact strength with variation in weight ratio of the DCP/TAIC content in the same matrix blends of PP/SBS (50/50). [Color figure can be viewed in the online issue, which is available at wileyonlinelibrary.com.]
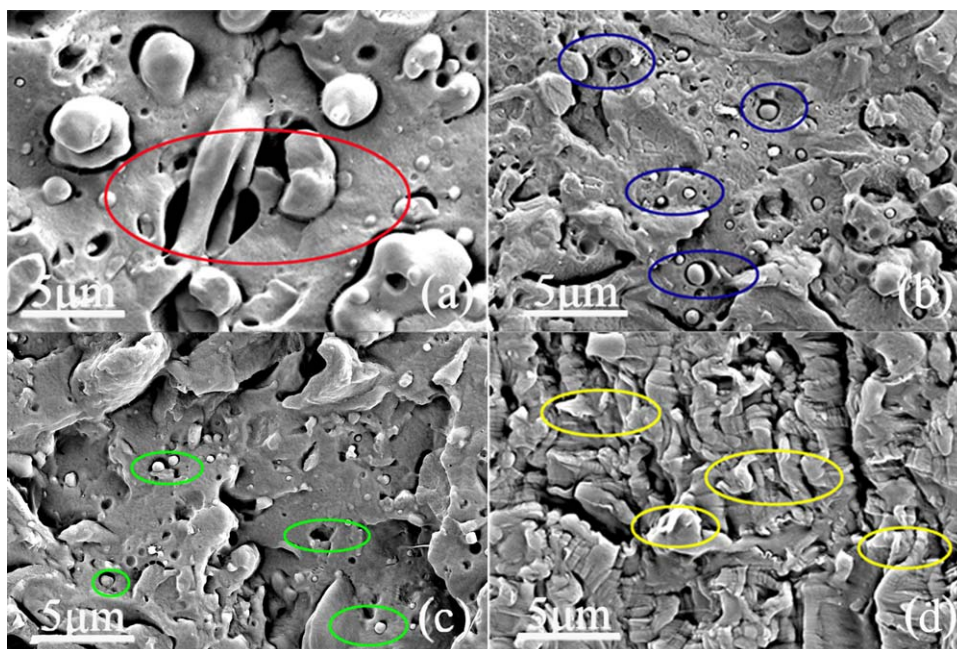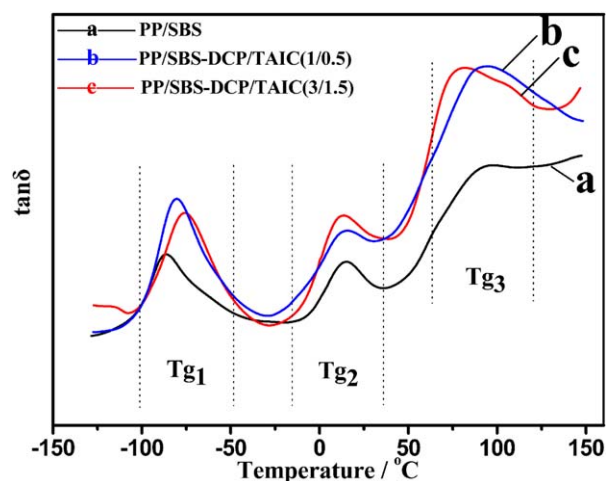
Figure 9. Morphology of the impact-fractured surfaces: (a) PP/SBS (50/50), (b) PP/SBS/DCP/TAIC (50/50/0.5/0.25),(c) PP/SBS/DCP/TAIC (50/50/1.0/0.50), (d) PP/SBS/DCP/TAIC (50/50/1.5/0.75). [Color figure can be viewed in the online issue, which is available at wileyonlinelibrary.com.]

observed that intensive plastic deformation occurred during the Izod impact, but no overlarge voids, naked debonding or spherical dispersed particles could be seen. This phenomenon suggested that the interfacial grafted structure can avoid the rupture of dispersed particles under tensile stress, and prevent debonding from occurring, ensure stress transfer between dispersed particles and polymer matrix. This phenomenon was in accordance to the plastic deformation mechanism.[42] Thus, the deformation progress of interfacial grafted copolymers could absorb plenty of fracture energy and improve greatly the notched Izod impact strength. However, in the impact-fractured surface of PP/SBS/DCP/TAIC (50/50/0.5/0.25) and PP/SBS/DCP/TAIC (50/50/1.0/0.50) blends in Figure 9(b,c), we could still find some SBS dispersed particles stripped from matrix of PP, forming a smooth, obvious interface within the substrate. This demonstrated the effects from interphase grafting were not as influential as the PP/SBS/DCP/TAIC (50/50/1.5/0.75) group. Comparing the cryofractured surface and impact-fractured surface morphologies in Figures 4(b,d) and 9(b,d), we can see the reactive compatibilization effect at a higher content is more prominent than lower content.

The reason for the loss on mechanical properties of PP/SBS (50/50) blend treated with lower contents (1.0–2.0 phr) of DCP/TAIC, could be the dominant effect from the chain scission of PP, which probably ruled out the effect from interfacial grafting. However, when adding the initiators higher to 3.0 phr, the interfacial grafting reaction contributed to a remarkable final increase on elongation at break and impact behavior.[20] Beyond that, the vulcanization of dispersed SBS phase and better compatibilization effect between components were also beneficial for mechanical performance, especially for the impact behaviors.

Dynamic Mechanical Analysis

DMA data for blends may provide information about glass transition temperatures of components to give better observation on the compatibility and interphase mixing of the blends. Plots of loss factor (tan δ) as a function of temperature for neat PP/SBS blend and reactive compatibilized blends are given in Figure 10, related T_g values can be seen in Table IV. Over the experimental temperature range, all the three samples exhibited three peaks, which represented the T_g of PP phase, PB segments and PS segments in SBS, respectively.

Figure 10. Loss factor (tan δ) versus temperature of different samples: (a) PP/SBS (50/50), (b) PP/SBS/DCP/TAIC (50/50/0.5/0.25), (c) PP/SBS/DCP/TAIC (50/50/1.5/0.75). [Color figure can be viewed in the online issue, which is available at wileyonlinelibrary.com.]

Table IV. T_g Values of Neat and Reactive Blends

| Samples	T_{g1} (°C)	T_{g2} (°C)	T_{g3} (°C)	ΔT_g between T_{g1} and T_{g2} (°C)
E#	−86.6	16.0	95.5	102.6
1#	−80.8	15.6	95.3	96.4
3#	−76.5	13.8	81.9	90.3

E# : PP/SBS (50/50), 1# : PP/SBS/DCP/TAIC (50/50/0.5/0.25), 3# : PP/SBS/DCP/TAIC (50/50/1.5/0.75).
T_{g1} represented for the PB segments in SBS; T_{g2} represented for the PP rich-phase; and T_{g3} represented for the PS segments in SBS.

As been proved above, the reaction in these blends was between the "double-bond" in PB segments and PP, the interphase *in situ* grafted copolymers structure would contribute a lot to the compatibility between these originally immiscible phases. We could observe the T_g of PP rich phase and the PB segments shifted closer, and ΔT_g was getting smaller from 102.6 to 90.3°C when increasing DCP content to 3.0 phr. These showed an enhancement of the compatibility between PP and SBS especially with 3.0 phr content of DCP/TAIC. The shifts of T_g values may imply also degradation of PP and crosslinking of SBS by interaction with DCP. Higher increase of T_g (SBS) than decrease of the T_g (PP), also implies crosslinking due to interaction of DCP with carbon double bond in soft SBS domains. Degradation and crosslinking processes were also additional possibilities for the DMA results.

Degradation Reaction versus Grafted Reaction
For a better confirmation of the competing effects from degradation and interfacial grafting reactions, thermal stability of initiator treated blends were studied. As we know the most common and direct method to observe the degradation of polymer molecular is through gel permeation chromatography (GPC), but in this research, GPC test was not introduced because of the extremely critical testing condition for PP/SBS blends. Compared to GPC test, thermal gravity analysis (TGA)
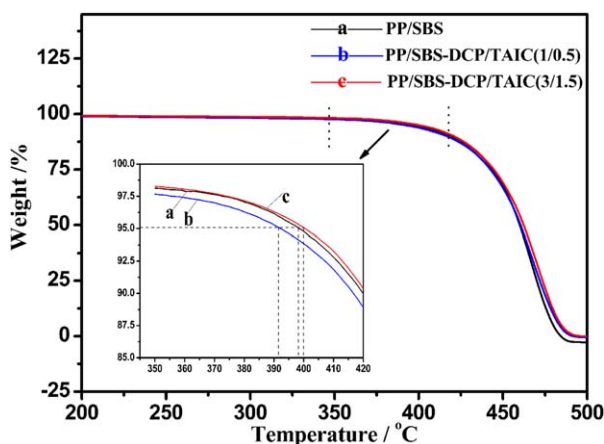
Figure 11. Thermal stability curves samples: (a) PP/SBS (50/50), (b) PP/SBS/DCP/TAIC (50/50/0.5/0.25), (c) PP/SBS/DCP/TAIC (50/50/1.5/0.75). [Color figure can be viewed in the online issue, which is available at wileyonlinelibrary.com.]
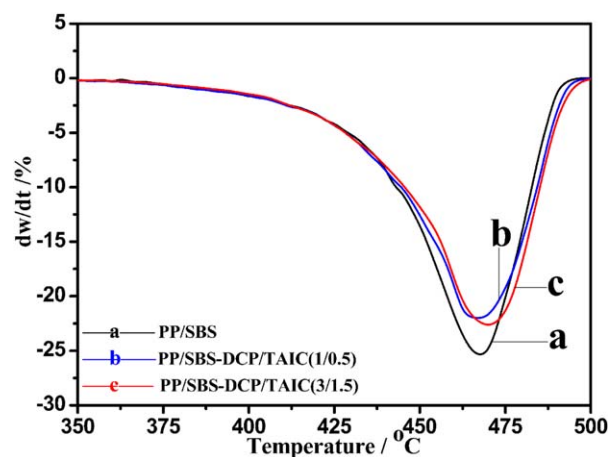
Figure 12. The integral and derivative thermogravimetric curves: (a) PP/SBS (50/50), (b) PP/SBS/DCP/TAIC (50/50/0.5/0.25), (c) PP/SBS/DCP/TAIC (50/50/1.5/0.75). [Color figure can be viewed in the online issue, which is available at wileyonlinelibrary.com.]

observation, which was also closely related to the molecular structure of samples, was easier to conduct. As shown in Figure 11, TGA of neat PP/SBS (50/50) blend and modified blends with various contents of DCP/TAIC was observed. The integral and derivative thermogravimetric curves in Figure 12 provide information about the temperature of maximum rates of mass losses (T_{-max}) for neat PP/SBS (50/50) blend, PP/SBS/DCP/TAIC (50/50/0.5/0.25) and PP/SBS/DCP/TAIC (50/50/1.5/0.75) blend. The temperatures at 5% weight loss ($T_{-0.05}$) as well as the temperature of maximum rates of mass losses (T_{-max}) had been listed in Table V. As one can see, the $T_{-0.05}$ and T_{-max} of PP/SBS (50/50) blend treated with 1.0 phr DCP/TAIC are lower than those of neat PP/SBS (50/50) blend, whereas when treated with 3.0 phr DCP/TAIC, the $T_{-0.05}$ (400.0°C) and T_{-max} (470.2°C) increased higher than those of neat blend ($T_{-0.05}$ =398.5°C, T_{-max} =467.5°C). Therefore, the order of thermal stability of these three samples should be: PP/SBS/DCP/TAIC (50/50/1.5/0.75) > PP/SBS (50/50) > PP/SBS/DCP/TAIC (50/50/0.5/0.25) blend. Owing to the predominant degradation effect in 1.0phr DCP/TAIC treated system, smaller molecular weight of PP chains were not resistant to heat, thus the sample showed the worst thermal stability. Once the degradation reaction was ruled out by the interfacial grafted reaction with the presence of 3.0 phr DCP/TAIC, the PP-grafted-SBS structure or the self-vulcanized SBS phase enabled the blend to be more stable on heat, led to an improvement on thermal stability. These results were consistent with mechanical properties.

Table V. Several Related Temperatures of Thermal Degradation of Neat and Reactive Blends

Samples	$T_{-0.05}$ (°C)	T_{-max} (°C)
E#	398.5	467.5
1#	392.0	466.1
3#	400.0	470.2

CONCLUSIONS

Initiator system DCP/TAIC with a fixed ratio was mixed with originally immiscible blends PP/SBS on self-designed VE. Torque curves proved the occurrence of interphase grafting reaction between PP and SBS, whereas the vulcanization reaction of SBS phase and degradation on PP phase could not be eliminated. Cryofractured surface morphologies of reactive compatibilized blends showed a reduction of dispersed particle sizes and an increment on interfacial adhesion, especially for PP/SBS/DCP/TAIC (50/50/1.5/0.75) blend. Owing to high level of interfacial grafted reaction, an enhancement on intercompatibility between two phases was achieved. Blends treated with lower contents of DCP/TAIC at 1.0–2.0 phr suffered a loss on mechanical performance compared to neat blend. However, when increasing DCP/TAIC initiator system to 3.0 phr, the blend showed a final enhancement on both tensile and impact properties higher than those of neat blend. The failure mode changed from debonding mechanism of neat 50PP/50SBS blend to plastic deformation mechanism of PP/SBS/DCP/TAIC (50/50/1.5/0.75) blend containing 3.0 phr initiator system, due to the strong interfacial strength. The loss factor (tan δ) analysis showed that DCP/TAIC improved the compatibility of PP and SBS. Both mechanical performance and thermal stability indicated that degradation effect of PP matrix was predominant in 1.0–2.0 phr DCP/TAIC treated system, then was ruled out by the interfacial grafted reaction when increasing DCP/TAIC to 3.0 phr, leading to an improvement on both mechanical properties and thermal stability. The reasons how the dominant factor changed with increasing content of DCP/TAIC initiator system, or the exact intergrafting degree in these experiments would continue to be studied. On our previous study, this article will leave useful reference or guidance to the reactive processing on VE. A supertough PP/SBS blend with enhanced tensile strength and thermal stability was obtained via this reactive compatibilization method.

REFERENCES

1. Jang, B. Z.; Uhlmann, D. R.; Vander Sande, J. B. *J. Appl. Polym. Sci.* **1985**, *30*, 2485.

2. Yokoyama, Y.; Ricco, T. *Polymer* **1998**, *39*, 3675.

3. Wei, G. X.; Sue, H. *J. Polym. Eng. Sci.* **2000**, *40*, 1979.

4. Van der Wal, A.; Nijhof, R.; Gaymans, R. *J. Polymer* **1999**, *40*, 6031.

5. Van der Wal, A.; Gaymans, R. *J. Polymer* **1999**, *40*, 6045.

6. Lin, Y.; Yakovleva, V.; Chen, H.; Hiltner, A.; Baer, E. *J. Appl. Polym. Sci.* **2009**, *113*, 1945.

7. Pracella, M.; Chionna, D.; Pawlak, A.; Galeski, A. *J. Appl. Polym. Sci.* **2005**, *98*, 2201.

8. Wilhelm, H. M.; Felisberti, M. I. *J. Appl. Polym. Sci.* **2003**, *87*, 516.

9. Wilhelm, H. M.; Felisberti, M. I. *J. Appl. Polym. Sci.* **2002**, *85*, 847.

10. Wilhelm, H. M.; Felisberti, M. I. *J. Appl. Polym. Sci.* **2002**, *86*, 359.

11. Hernández, M.; Ichazo, M. N.; González, J.; Albano, C.; Santana, O. *Adv. Mater. Res.* **2008**, *47*, 278.

12. Saroop, M.; Mathur, G. N. *J. Appl. Polym. Sci.* **1997**, *65*, 2691.

13. Van Aert, H. A. M.; Van Steenpaal, G. J. M.; Nelissen, L. N. I. H.; Lemstra, P. J.; Liska, J.; Bailly, C. *Polymer* **2001**, *42*, 2803.

14. Crevecoeur, J. J.; Nelissen, L. N. I. H.; Van der Sanden, M. C. M.; Lemstra, P. J.; Mencer, H. J.; Hogt, A. H. *Polymer* **1995**, *36*, 753.

15. Tuba, F.; Oláh, L.; Nagy, P. *Eng. Fract. Mech.* **2011**, *78*, 3123.

16. Harada, M.; Iida, K.; Okamoto, K.; Hayashi, H.; Hirano, K. *Polym. Eng. Sci.* **2008**, *48*, 1359.

17. Coltelli, M. B.; Toncelli, C.; Ciardelli, F.; Bronco, S. *Polym. Degrad. Stabil.* **2011**, *96*, 982.

18. Kim, B. K.; Do, I. H. *J. Appl. Polym. Sci.* **1996**, *61*, 439.

19. Inoue, T.; Suzuki, T. *J. Appl. Polym. Sci.* **1995**, *56*, 1113.

20. Ludwig, K. N.; Moore, R. B. *J. Elastom. Plast.* **2002**, *34*, 171.

21. Kim, K. H.; Cho, W. J.; Ha, C. S. *J. Appl. Polym. Sci.* **1996**, *59*, 407.

22. Scott, C. E.; Macosko, C. W. *Polymer* **1995**, *36*, 461.

23. Utracki, L. A.; Shi, Z. H. *Polym. Eng. Sci.* **1992**, *32*, 1824.

24. Scott, C. E.; Macosko, C. W. *Polym. Bull.* **1991**, *26*, 341.

25. Rauwendaal, C.; Osswald, T.; Gramann, P.; Davis, B. *Int. Polym. Proc.* **1999**, *14*, 28.

26. Chiba, K.; Nakamura, K. *J. Non-Newton. Fluid.* **1998**, *78*, 167.

27. Nguyen, X. Q.; Ormeaux, D.; Utracki, L. A. U. S. Patent 5, 4511, 06A **1995**.

28. Qu, J. P. CN. Patent 200810026054.X **2008**.

29. Qu, J. P.; Liu, L. M.; Tan, B.; Liu, S. R.; Chen, H. X.; Feng, Y. H. *Polym. Compos.* **2012**, *33*, 185.

30. Kim, Y.; Cho, W. J.; Ha, C. S.; Kim, W. *Polym. Eng. Sci.* **1995**, *35*, 1592.

31. Zhao, W.; Wu, G.; Yang, Q. *Polym.-Plast. Technol.* **2012**, *51*, 716.

32. Zhao, Y.; Huang, H. X.; Chen, Y. K.; Wu, X. J. *J. Mater. Sci.* **2010**, *45*, 4054.

33. Inoue, T. *J. Appl. Polym. Sci.* **1994**, *54*, 709.

34. Qu, J. P.; Chen, H. Z.; Liu, L. S. *J. Appl. Polym. Sci.* **2013**, *128*, 3576.

35. Shieh, Y. T.; Liao, T. N.; Chang, F. C. *J. Appl. Polym. Sci.* **2001**, *79*, 2272.

36. Wilhelm, H. M.; Felisberti, M. I. *J. Appl. Polym. Sci.* **2002**, *86*, 366.

37. Coltelli, M. B.; Bronco, S.; Chinea, C. *Polym. Degrad. Stabil.* **2010**, *95*, 332.

38. Paul, S.; Kale, D. D. *J. Appl. Polym. Sci.* **2000**, *76*, 1480.

39. Ichazo, M.; Hernandez, M.; Gonzalez, J.; Albano, C.; Dominguez, N. *Polym. Bull.* **2004**, *51*, 419.

40. Kim, G. M.; Michler, G. H. *Polymer* **1998**, *39*, 5699.

41. Pawlak, A.; Galeski, A.; Rozanski, A. *Prog. Polym. Sci.* **2014**, *39*, 921.

42. Deblieck, R. A.; Van Beek, D. J. M.; Remerie, K.; Ward, I. M. *Polymer* **2011**, *52*, 2979.